# Binding energy and spatial extension of an off-centre donor impurity in ZnS/CdSe spherical core/shell nanostructures

A. IBRAL[a,b], A. ZOUITINE[c], EL MAHDI ASSAID[a,b], EL MUSTAPHA FEDDI[c], F. DUJARDIN[d]
[a]*Equipe d'Optique et Electronique du Solide, Département de Physique, Faculté des Sciences, Université Chouaïb Doukkali, B. P. 20 El Jadida principale, El Jadida, Royaume du Maroc.*
[b]*Laboratoire d'Instrumentation, Mesure et Contrôle, Département de Physique, Université Chouaïb Doukkali, B. P. 20 El Jadida principale, El Jadida, Royaume du Maroc.*
[c]*Département de Physique, Ecole Nationale Supérieure d'Enseignement Technique, Université Mohammed V Souissi, B. P. 6207 Rabat-Instituts, Rabat, Royaume du Maroc.*
[d]*LCPMC, Institut de Chimie, Physique et Matériaux, Université de Lorraine, 1 Bd Arago, 57070 Metz, France.*

Coulomb correlation, binding energy and inter-particle distance of a donor impurity placed anywhere in the well region of a spherical core/shell nanostructure are studied in the framework of the effective mass approximation. Finite height barrier is used to describe conduction band offset between core and shell of the structure. Electron effective mass mismatch between core and shell and dielectric mismatch at the surface where core and shell materials meet are taken into account. Off-centre donor ground state energy is determined via Ritz variational principle using a trial wave function where Coulomb attraction between electron and ionized donor is considered. The theoretical approach developed is used to determine Coulomb correlation parameter, binding energy and spatial extension of the off-centre donor as functions of core to shell radii ratio for ZnS/CdSe core/shell nanostructures immersed in aqueous or organic solution.

(Received November 11, 2014; accepted January 21, 2015)

*Keywords:* Off-centre donor, Exciton, Core/Shell nanostructure, Quantum dot, Dielectric mismatch

## 1. Introduction

The quantum size effects have been described, for the first time, in the early 80's by Alexei I. Ekimov [1] and Louis E. Brus [2, 3]. Since these original and pioneering works Quantum Dots (QD's) have been investigated widely both theoretically and experimentally. QD's are semiconductor inclusions which may be synthesized via soft chemistry methods at low temperature as colloidal suspensions in organic solutions, or precipitated at high temperature in a semiconducting or in an isolating host matrix. QD's are synthetic structures which are at the midway between solids and atoms. They present spatial order and compactness of bulk semiconductors, however their emission and absorption spectra are close to those of single atoms. In fact, because of ultimate confinement in three directions of space, all degrees of freedom of charge carriers are frozen. Due to their nanometer scale size, quantum characters of electrons and holes emerge, their energies are quantized and depend on the dot size. So, the line which corresponds to transition from top of valence band to bottom of conduction band is blue shifted and the absorption spectrum reduces to a series of narrow and intense peaks. This outstanding property enables tuning, in advance, effective gap of quantum dot which is known in literature under the name of ***''band gap engineering''***.

Nowadays, technological advances in the field of experimental techniques of growth have enabled fabrication of high-quality semiconductor QD's within a wide range of sizes for different fields of applications such as optical encryption [4], multiplexing [5], solar light harvesting in both the visible and the near infrared for hydrogen generation [6], biological and medical applications where QD's are used for sensing intracellular processes at the single molecule level [7,8]. They are also utilized as fluorescent tags in high-resolution cellular imaging [9-12], as relevant intracellular probes to investigate routing of ligands in live cell, in tumor targeting and in diagnostics [13-16].

In the two last decades, spatial attention devoted to QD's has in a large part shifted to Core/Shell nanostructures. These latter structures are similar to onion, they are also named Quantum Dot-Quantum Well structures [17], they involve, basically, lattice matched semiconductors. They are mostly obtained via soft chemistry processes of growth by coating a spherical quantum dot of a given semiconductor with a spherical shell of another semiconductor. This shell may also be encapsulated by a spherical organic or inorganic thin layer to smooth quantum dot surface and to neutralize dangling bonds. By virtue of conduction and valence band edges alignments of semiconductors concerned, the final nanostructure may be of type I when electrons and holes are confined in nanostructure core (CdSe/CdS [18], CdSe/ZnSe [19]) (see figure 1a), inverted type I when electrons and holes are confined in nanostructure shell

(CdS/CdSe [20], ZnSe/CdSe [21]) (see figure 1b), type II when charge carriers of opposite sign are spatially separated i.e. electrons are confined in core while holes are confined in shell of quantum dot (CdTe/CdSe [22], CdS/ZnSe [23]) or vice versa (see figure 1c). In core/shell nanostructures, electron and hole ground state energies as well as their radial probability densities depend on core and shell geometrical parameters. This exceptional property enables tuning, in advance, effective gap of nanostructure and single particles radial probabilities of presence inside the dot which is known in literature under the name of ***''wave function engineering''***.

According to present status of science and technology, colloidal solutions from soft chemistry methods containing semiconducting core/shell nanostructures as suspensions exhibit outstanding spectroscopic properties. Their electroluminescence and photoluminescence spectra depend on semiconductors involved, on core size and shell thickness which enables synthesis of quantum dot size-tunable color colloidal solution, fabrication of electrically driven colloidal quantum dot light emitting devices (QD-LED) and electrically driven full-color QD-LED displays [24].

Shallow impurities whose energy levels are close to bottom of conduction band or top of valence band are expected to play a key role in emission or absorption of core/shell nanostructures. In past few years, some theoretical works were devoted to stark effect [25] and diamagnetic effect [26] on off-centre donor binding energy respectively in a spherical quantum dot and in a spherical quantum dot-quantum well. This year, diamagnetic susceptibility of an off-centre donor [27] and polarizability of an on-centre donor impurity confined in a core/shell nanostructure were calculated in the framework of the effective mass approximation. It appears that application of an external electric field leads to a weakening of hydrogen-like donor binding while application of a magnetic field implies a strengthening of attraction between opposite sign particles.

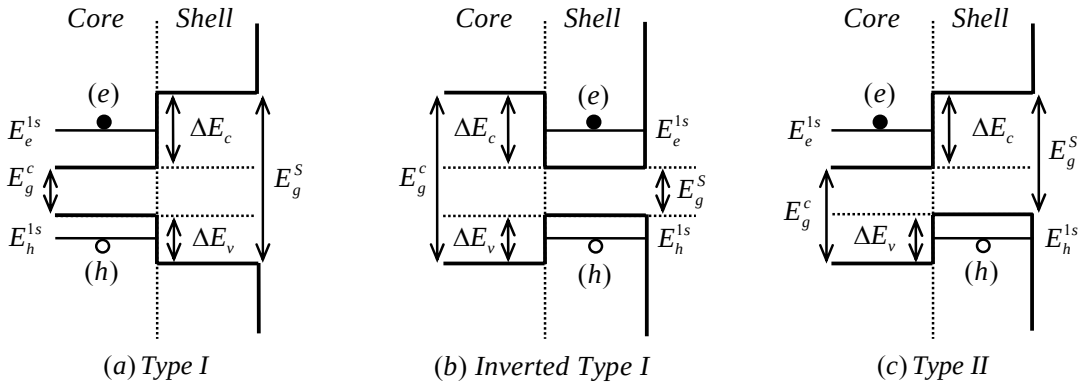


*Figs. 1. Conduction and valence band offsets for type I (a), inverted type I (b) and type II spherical core/shell nanostructures.*

In this study, we determine ground state energy and wave function of an electron confined in a spherical core/shell nanostructure. We show that for a fixed dot radius $R_S$, it exists a critical value $R_{Ce}$ of core radius for which electron energy $E_e^{1s}$ is equal to conduction band offset $V_{0e}$ (see figure 2b). So for $0 < R_C < R_{Ce}$, electron energy $E_e^{1s}$ is lighter than conduction band offset $V_{0e}$ while electron wave function is standing in shell and is evanescent in core (see figure 2a). On the other hand for $R_{Ce} < R_C < R_S$, electron energy $E_e^{1s}$ is greater than conduction band offset $V_{0e}$ whereas electron wave function is standing in the whole nanostructure (see figure 2c). On the basis of electron wave function expressions, we construct a trial wave function for off-centre donor which takes into account attractive Coulomb correlation between opposite sign particles. Then, we determine via Ritz variational principle ground state energy, binding energy, Coulomb correlation parameter and spatial extension of a donor placed anywhere in the well region of a spherical core/shell nanostructure as functions of core to shell radii ratio for different ionized donor positions.

## 2. Theory

Let us consider an off-centre donor placed in the well region of an inverted type I core/shell hetero-nanostructure (see figure 1b). This kind of structure is composed by a spherical wide band gap semiconductor nanocrystal of radius $R_C$ and a dielectric constant $\varepsilon_1$ playing the role of core, over coated with a narrower band gap semiconductor layer of a radius $R_S$, a thickness $T = R_S - R_C$ and a dielectric constant $\varepsilon_2$ playing the role of a shell. The whole nanostructure is immersed in an aqueous or in an organic solution. The bottom of core conduction band is above the bottom of shell conduction band (see figure 1b). The top of core valence band is below the top of shell valence band (see figure 1b). Due to this well-like band

profiles, charge carriers are partially confined in narrowest band gap semiconductor.

### 2.1 Electron ground state energy and wave function

In the framework of the effective mass approximation and assuming isotropic, parabolic and non-degenerated bands, the Hamiltonian $H_e$ of a confined electron, in CGS electrostatic units, reads:

$$H_e = (\frac{\hbar}{j}\nabla_e)\frac{1}{2m_e^*(r_e)}(\frac{\hbar}{j}\nabla_e) + V_{we}(r_e) \quad (1)$$

The first term stands for hermitian kinetic energy operator for a position dependent effective mass particle proposed for the first time by BenDaniel and Duke [28].

Electron effective mass in unit of free electron mass $m_0$ is given by:

$$m_e^*(r_e) = \begin{cases} m_{e1}^*, & r_e < R_C \\ m_{e2}^*, & R_C < r_e < R_S \end{cases} \quad (2)$$

$R_C$ and $R_S$ are respectively inner and outer radii of core/shell nanostructure (see figures 2).

Electron confining potential inside narrowest band gap semi-conductor due to conduction band offset between core, shell and host medium $V_{we}(r_e)$ is expressed as follows:

$$V_{we}(r_e) = \begin{cases} V_{0e}, & 0 < r_e < R_C \\ 0, & R_C < r_e < R_S \\ \infty, & R_S < r_e \end{cases} \quad (3)$$

The Schrödinger equation giving electron eigenvalues $E_e$ and eigenfunctions $\Psi_e(\vec{r_e})$ writes:

$$H_e\ \Psi_e(\vec{r_e}) = E_e\ \Psi_e(\vec{r_e}) \quad (4)$$

Separation of radial and angular variables in equation (4) leads to the following expression of wave functions:

$$\Psi_e(\vec{r_e}) = R_e^{n,l}(r_e)\, Y_{l,m}(\theta_e, \varphi_e) \quad (5)$$

$R_e^{n,l}(r_e)$ is the radial part of wave functions, $Y_{l,m}(\theta_e, \varphi_e)$ is a spherical harmonic, $n$ is the principal quantum number, $l$ and $m$ are orbital and magnetic quantum numbers.

Afterwards, we focus on electron ground state corresponding to following quantum numbers $n=1$, $l=0$ and $m=0$, namely 1s state since nanostructure effective gap is related to shell semiconductor gap by the following equation:

$$E_g^{Core/Shell} = E_g^{Shell} + E_e^{1s} + E_h^{1s} \quad (6)$$

To determine the radial part $R_e^{1s}(r_e)$ of an electron wave function for all values of core radius $R_C$ lying between 0 and a predetermined shell size $R_S$, one must consider two different cases. In the first one, electron ground state energy $E_e^{1s} < V_{0e}$ and core radius $R_C < R_{Ce}$ where $R_{Ce}$ is a critical value of $R_C$ corresponding to $E_e^{1s} = V_{0e}$ (see figure 2.1). Maximum of radial probability density function is in shell and radial part $R_e^{1s}(r_e)$ of electron wave function writes :

$$R_e^{1s}(r_e) = \begin{cases} A_{1e}\dfrac{sh(k_{1e}r_e)}{r_e}, & 0 < r_e < R_C \\ A_{2e}\dfrac{\sin(k_{2e}(r_e - R_S))}{r_e}, & R_C < r_e < R_S \end{cases} \quad (7)$$

where $k_{1e} = \sqrt{2m_{1e}^*(V_{0e} - E_e)/\hbar^2}$ and $k_{2e} = \sqrt{2m_{2e}^* E_e/\hbar^2}$. In the second case, $E_e^{1s} > V_{0e}$ and $R > R_{Ce}$. Maximum of probability density function is in core and radial part $R_e^{1s}(r_e)$ of single particle wave function reads:

$$R_e^{1s}(r_e) = \begin{cases} A_{3e}\dfrac{\sin(k_{3e}r_e)}{r_e}, & 0 < r_e < R_C \\ A_{4e}\dfrac{\sin(k_{4e}(r_e - R_S))}{r_e}, & R_C < r_e < R_S \end{cases} \quad (8)$$

where $k_{3e} = \sqrt{2m_{1e}^*(E_e - V_{0e})/\hbar^2}$ and $k_{4e} = \sqrt{2m_{2e}^* E_e/\hbar^2}$. In each case, the coefficients $A_{je}$ are determined via normalization condition:

$$\int_0^{R_S} \left(R_e^{1s}(r_e)\right)^2 4\pi r_e^2 dr_e = 1 \quad (9)$$

and continuity condition of radial part of wave function $R_e^{1s}(r_e)$ at core surface ( $r_e = R_C$ ) :

$$R_{Core,e}^{1s}(r_e)\Big)_{r_e=R_C} = R_{Shell,e}^{1s}(r_e)\Big)_{r_e=R_C} \quad (10)$$

Electron ground state energy $E_e^{1s}$ is determined by solving numerically the transcendental equation obtained by combining continuity conditions of radial part of wave function $R_e^{1s}(r_e)$ and probability current density at core surface ( $r_e = R_C$ ):

$$\frac{1}{m_{1e}^*}\frac{dR_{Core,e}^{1s}(r_e)}{dr_e}\Big)_{r_e=R_C} = \frac{1}{m_{2e}^*}\frac{dR_{Shell,e}^{1s}(r_e)}{dr_e}\Big)_{r_e=R_C} \quad (11)$$

For a given value $R_S$ of nanostructure size, the transcendental equation giving critical value of core radius $R_{C,e}$ for which $E_e^{1s} = V_{0e}$ is given by:

$$\left(R_C\sqrt{2m_{2e}^{*}V_{0e}/\hbar^2}\cot((R_C-R_S)\sqrt{2m_{2e}^{*}V_{0e}/\hbar^2})\right)-1=0 \quad (12)$$

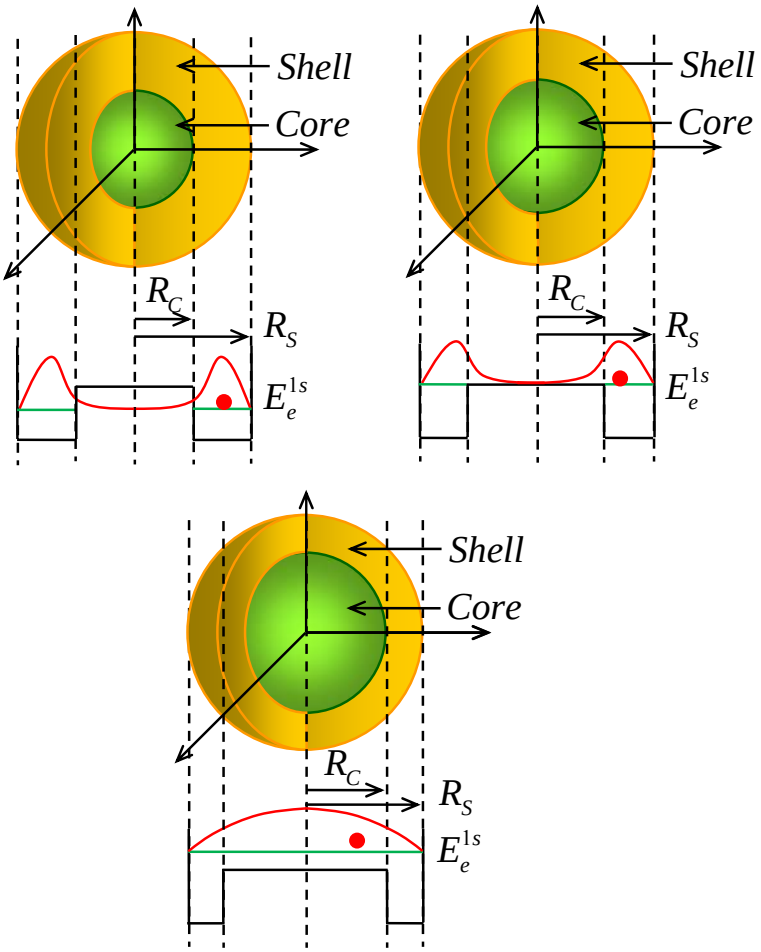


*Fig. 2: Inverted type I ZnS/CdSe core/shell nanostructures for a fixed shell size and different core radii : (2.1) $R_C < R_{Ce}$ and $E_e^{1s} < V_{0e}$, (2.2) $R_C = R_{Ce}$ and $E_e^{1s} = V_{0e}$, (2.3) $R_C > R_{Ce}$ and $E_e^{1s} > V_{0e}$.*

### 2.2 Off-centre donor ground state energy and wave function:

In CGS electrostatic units and under the same assumptions as for a single particle, the Hamiltonian of an off-centre donor placed in well region and on z-axis writes:

$$H_{D^0} = -\frac{\hbar^2\Delta_e}{2m_e^{*}(r_e)} + V_{we}(r_e) - \frac{e^2}{\varepsilon(r_e,d)\sqrt{r_e^2+d^2-2r_e d\cos(\theta_e)}} \quad (13)$$

$e$ is the elementary charge. $d$ is the ionized donor distance to quantum dot centre such as $R_C < d < R_S$. In our study, we focus on ZnS/CdSe nanostructures. These lattice matched semiconductors crystallize in the same Bravais lattices (hexagonal wurtzite and cubic zincblende), their dielectric constants are very close (see Table 1) which allow to ignore the effects of induced surface polarization charges. In these conditions, electron and ionized donor positions dependent dielectric constant $\varepsilon(r_e,d)$ reads:

$$\varepsilon(r_e,d) = \begin{cases} \varepsilon_2, & R_C < r_e < R_S \text{ and } R_C < d < R_S \\ (\varepsilon_1+\varepsilon_2)/2, & 0 < r_e < R_C \text{ and } R_C < d < R_S \end{cases} \quad (14)$$

Electron Hamiltonian presents the spherical symmetry but off-centre donor Hamiltonian presents the cylindrical symmetry. So, off-centre donor wave function must be expressed in Hylleraas coordinates $r_e, d$ and $r_{e-D^+}$. Within this coordinates system, the Laplacian operator writes :

$$\Delta_e = \frac{\partial^2}{\partial r_e^2} + \frac{2}{r_e}\frac{\partial}{\partial r_e} + \frac{r_e^2 - d^2 + r_{e-D^+}^2}{r_e r_{e-D^+}}\frac{\partial^2}{\partial r_e \partial r_{e-D^+}} + \frac{\partial^2}{\partial r_{e-D^+}^2} + \frac{2}{r_{e-D^+}}\frac{\partial}{\partial r_{e-D^+}} \quad (15)$$

Off-centre donor ground state energy and associated wave function are solutions of the effective Schrödinger equation :

$$H_{D^0}\Psi_{D^0}(r_e,d,r_{e-D^+}) = E_{D^0}\Psi_{D^0}(r_e,d,r_{e-D^+}) \quad (16)$$

Equation (16) is not solvable analytically. To determine its ground state solutions, we need to use an approximation method. Here, we use Ritz variational principle and choose the following trial wave function:

$$\Psi_{D^0}(r_e,d,r_{e-D^+}) = R_e^{1s}(r_e)\exp(-\alpha\, r_{e-D^+}) \quad (17)$$

$R_e^{1s}(r_e)$ is the electron wave function given in section 2.1. In equation (17), exponential factor is introduced in order to take into account Coulomb attraction between electron and ionized off-centre donor. $\alpha$ is a variational parameter. Off-centre donor ground state energy $E_{D^0}$ is obtained by minimization of the expectation value of $H_{D^0}$ with respect to $\alpha$ :

$$E_{D^0} = \min_{\alpha}\frac{\left\langle \Psi_{D^0}\left| H_{D^0}\right|\Psi_{D^0}\right\rangle}{\left\langle \Psi_{D^0}\left|\Psi_{D^0}\right.\right\rangle} \quad (18)$$

Finally, off-centre donor binding energy $E_b$ is expressed as follows :

$$E_b = E_e^{1s} - E_{D^0} \quad (19)$$

To lighten single particle Hamiltonian (equation 1) and off-centre donor Hamiltonian (equation 13), and to compare with the results of an exciton confined in a ZnS/CdSe core/shell nanostructure, we use as unit of length $a_X^* = \bar{\varepsilon}\hbar^2/e^2\bar{\mu} = 2.7378\ nm$ , which represents heavy-hole-exciton effective Bohr radius in an intermediate bulk material between ZnS and CdSe (see Table 1) and as unit of energy $R_X^* = \bar{\mu}e^4/2\bar{\varepsilon}^2\hbar^2 = 28.7311\ meV$ , which represents absolute value of heavy-hole-exciton ground state energy in intermediate bulk material between ZnS and CdSe (see Table 1). $\bar{\varepsilon} = (\varepsilon_1+\varepsilon_2)/2$ is the mean relative dielectric constant. $\bar{\mu} = \overline{m_e^*}\,\overline{m_h^*}/(\overline{m_e^*}+\overline{m_h^*})$ is the reduced mass of exciton in intermediate bulk material. $\overline{m_i^*} = (\overline{m_{i1}^*}+\overline{m_{i2}^*})/2$ $(i = e, h)$ are single particles mean effective masses.

*Table 1: ZnS and CdSe physical parameters used in the numerical calculations.*

| | *ZnS* | *CdSe* | *Intermediate bulk material* |
|---|---|---|---|
| $m_e^*/m_0$ | 0.28 [29] | 0.13 [29] | 0.205 |
| $m_h^*/m_0$ | 1.40 [29] | 1.17 [29] | 1.285 |
| $\mu$ | 0.2333 | 0.117 | 0.1767 |
| $E_g\,(eV)$ | 3.81 [29] | 1.75 [29] | |
| $\varepsilon/\varepsilon_0$ | 8.9 [30] | 9.4 [30] | 9.15 |
| $a_X^*\,(nm)$ | 2.0177 | 4.2500 | 2.7378 |
| $R_X^*\,(meV)$ | 40.0793 | 18.0158 | 28.7311 |

## 3. Results and discussions

In what follows, Ritz variational principle is used to determine the ground state energy and the corresponding wave function of an off-centre donor confined in a ZnS/CdSe core/shell nanostructure. Conduction band offset $\Delta E_c$ between core and shell is modeled by a finite height barrier. Electron effective mass mismatch at the boundary between core and shell and dielectric constant mismatch between core and shell materials are considered. Variational parameter $\alpha$, binding energy $E_b$, spatial extension $\left\langle r_{e-D^+}\right\rangle$ and radial probability density $r_e^2\Psi_{D^0}^2$ of a donor placed anywhere in the well region of a ZnS/CdSe core/shell nanostructure are determined as functions of the core to shell radii ratio $R_C/R_S$ for different ionized donor positions $d$ inside the well of the structure.

In figures (3.1), (3.2) and (3.3), variations of Coulomb correlation parameter $\alpha$, binding energy $E_b$ and inter-particle distance $\left\langle r_{e-D^+}\right\rangle$ of a hydrogenic donor are drawn against core to shell radii ratio $R_C/R_S$ for a shell radius $R_S = 4$ ex. units and for three donor positions : $d = R_C$ (red lines), $d = (R_C+R_S)/2$ (green lines), $d = R_S$ (blue lines) and in the case of heavy-hole exciton (magenta lines) [31]. Solid lines and dashed lines correspond to cases where dielectric mismatch between core and shell materials is taken into account ( $\varepsilon_1 = 8.9$ , $\varepsilon_2 = 9.4$ ) and ignored ( $\varepsilon_1 = \varepsilon_2 = 9.15$ ) respectively.

In figures 4, off-centre donor radial probability density $r_e^2\Psi_{D^0}^2$ is plotted for a shell radius $R_S = 4$ ex. units, different values of core radius $R_C$ and three donor positions : $d = R_C$, $d = (R_C + R_S)/2$ and $d = R_S$.

We begin by the comment of figures 3. First of all, we fix shell radius value and discuss the effect of core radius. One can remark that Coulomb correlation parameter $\alpha$ and binding energy $E_b$ curves show approximately the same behavior. However, inter-particle distance $\langle r_{e-D^+} \rangle$ shows an opposite behavior. To understand these behaviors we recall that in barrier/well structures such as ZnS/CdSe nanostructures, we have competition between tridimensional confinement in core which is predominant when core radius $R_C$ tends to 0 or to $R_S$, and bi-dimensional confinement in shell which is predominant for an intermediate shell thickness $T_S = R_S - R_C$ around 0.3 ex. units=0.82 nm [31]. So for $R_C = 0$, Coulomb correlation parameter and binding energy are minimum, inter-particle distance is maximum. These three physical quantities correspond, respectively, to $\alpha$, $E_b$ and $\langle r_{e-D^+} \rangle$ of a hydrogenic donor impurity in CdSe spherical quantum dot. When $R_C$ increases, Coulomb correlation parameter increases, binding energy increases too while inter-particle distance decreases. $\alpha$ and $E_b$ culminate at maximum values while $\langle r_{e-D^+} \rangle$ drops to a minimal value. These extreme values correspond to strongest bi-dimensional character of hydrogenic donor in a CdSe thin spherical layer of thickness around 0.3 ex. units=0.82 nm [31], i.e. when radial probability density of hydrogenic donor in well is maximum and hydrogenic donor cloud is sandwiched between core and matrix. Next, Coulomb correlation parameter decreases, binding energy decreases too while inter-particle distance increases. Each physical quantity tends to appropriate limit value corresponding to hydrogenic donor in ZnS spherical quantum dot.

As presented by figures 3, the three physical quantities $\alpha$, $E_b$ and $\langle r_{e-D^+} \rangle$ describe the correlation between opposite-sign particles. Indeed, for strongly correlated particles in a CdSe thin spherical layer, off-centre donor Coulomb correlation parameter and binding energy values are the highest, electron-ion distance is the lowest. However for weakly correlated particles, Coulomb correlation parameter and binding energy values are the lowest, electron-ion distance is the highest.

We have seen above that when $R_C$ tends to 0, core/shell nanostructure reduces to a CdSe spherical quantum dot. Now, we will discuss the ionized donor $D^+$ position effect on off-centre donor Coulomb correlation parameter $\alpha$, binding energy $E_b$ and spatial extension $\langle r_{e-D^+} \rangle$. For $D^+$ position such as $d = R_C$, our system reduces to an on-centre donor in a CdSe quantum dot (see figure (4. a. 1)), $\alpha$, $E_b$ and $\langle r_{e-D^+} \rangle$ tend to 0.48 ex. units, 1.43 ex. units and 1.51 ex. units respectively. These limit values are in good agreement with those found by Ekimov *et al.* [32, 33] and E. Assaid *et al.* [34]. For an ionized donor $D^+$ placed at $d = (R_C + R_S)/2$, the problem reduces to an off-centre donor at halfway between centre and surface of a CdSe quantum dot (see figure (4. a. 2)), $\alpha$, $E_b$ and $\langle r_{e-D^+} \rangle$ tend to 0.55 ex. units, 1.15 ex. units and 1.74 ex. units. Here, we recover the limit values found by E. Assaid *et al.* [34] and Nomura and Kobayashi [35]. For an ionized donor $D^+$ placed at $d = R_S$, the problem reduces to an on-surface donor in a CdSe quantum dot (see figure (4. a. 3)), $\alpha$, $E_b$ and $\langle r_{e-D^+} \rangle$ tend to 0.17 ex. units, 0.53 ex. units and 3.88 ex. units in accordance with the limit values found in references [34] and [35].

When $R_C$ tends to $R_S$, core/shell nanostructure reduces to a ZnS spherical quantum dot. For all ionized donor $D^+$ positions $d = R_C$, $d = (R_C + R_S)/2$ and $d = R_S$, our problem is equivalent to an on-surface donor in a ZnS quantum dot (see figures (4. d. 1), (4. d. 2) and (4. d. 3)), $\alpha$, $E_b$ and $\langle r_{e-D^+} \rangle$ tend to 0.5 ex. units, 0.60 ex. units and 3 ex. units. These limit values are in good agreement with those of references [34] and [35].

For a shell thickness $T_S = R_S - R_C \approx 0.3$ ex. units $(R_C / R_S = 0.92)$, off-centre donor is confined in a thin spherical layer of CdSe. Its behavior is similar to that of an off-centre donor in a quantum well (see figures (4.c.1), (4.c.2) and (4.c.3)). Coulomb correlation parameter and binding energy are maximal (see figures (3.1) and (3.2)) while inter-particle distance is minimal (see figure (3.3)).

In figure (3.2), we notice that for thin spherical layer of CdSe, $D^+$ position providing highest energy corresponds to $d = R_C$. This is due to geometric discomfort which is minimal in this position contrarily to position $d = R_S$ where electron cloud is pushed, by the barrier, far from $D^+$. We also notice that when $D^+$ moves from core surface to shell surface, electron cloud follows the nucleus $D^+$ and core radius value corresponding to highest energy increases slightly.

Comparing off-centre donor to heavy-hole exciton, one can remark that for core radius $R_C < R_{Ce}$ physical quantities of an off-centre donor at halfway between shell surfaces are close to that of heavy-hole exciton. In a first approximation, heavy-hole exciton can be described as a volume hydrogenic donor which reminds the concept of donor-like exciton proposed by Ekimov [36].

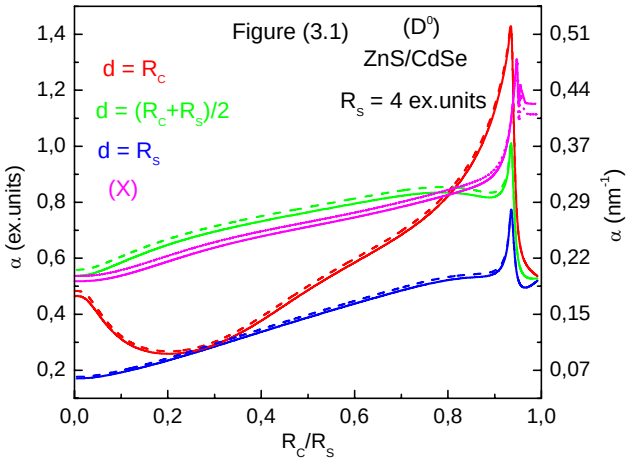


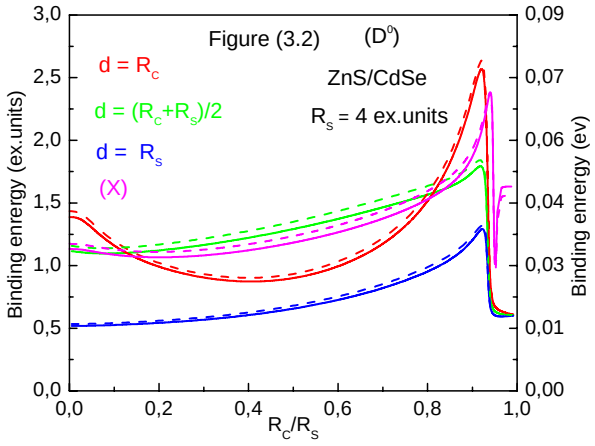


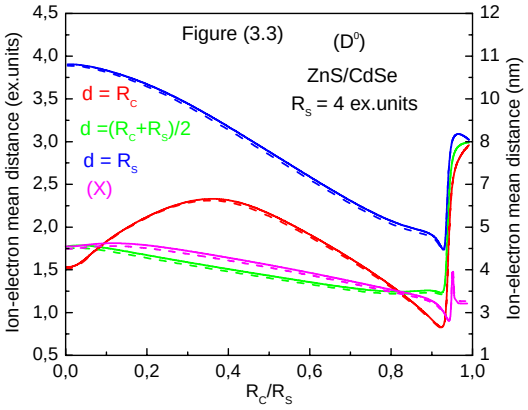


*Fig.3. Variational parameter* $\alpha$ *(3.1), binding energy* $E_b$ *(3.2) and spatial extension* $\left\langle r_{e-D^+} \right\rangle$ *(3.3) versus core to shell radii ratio* $R_C / R_S$ *of an off-centre donor confined in a ZnS/CdSe core/shell nanostructure with a shell radius* $R_S = 4$ *ex. units. Solid lines and dashed lines correspond to cases where dielectric mismatch between core and shell materials is taken into account (* $\varepsilon_1 = 8.9$ *,* $\varepsilon_2 = 9.4$ *) and ignored (* $\varepsilon_1 = \varepsilon_2 = 9.15$ *) respectively.*

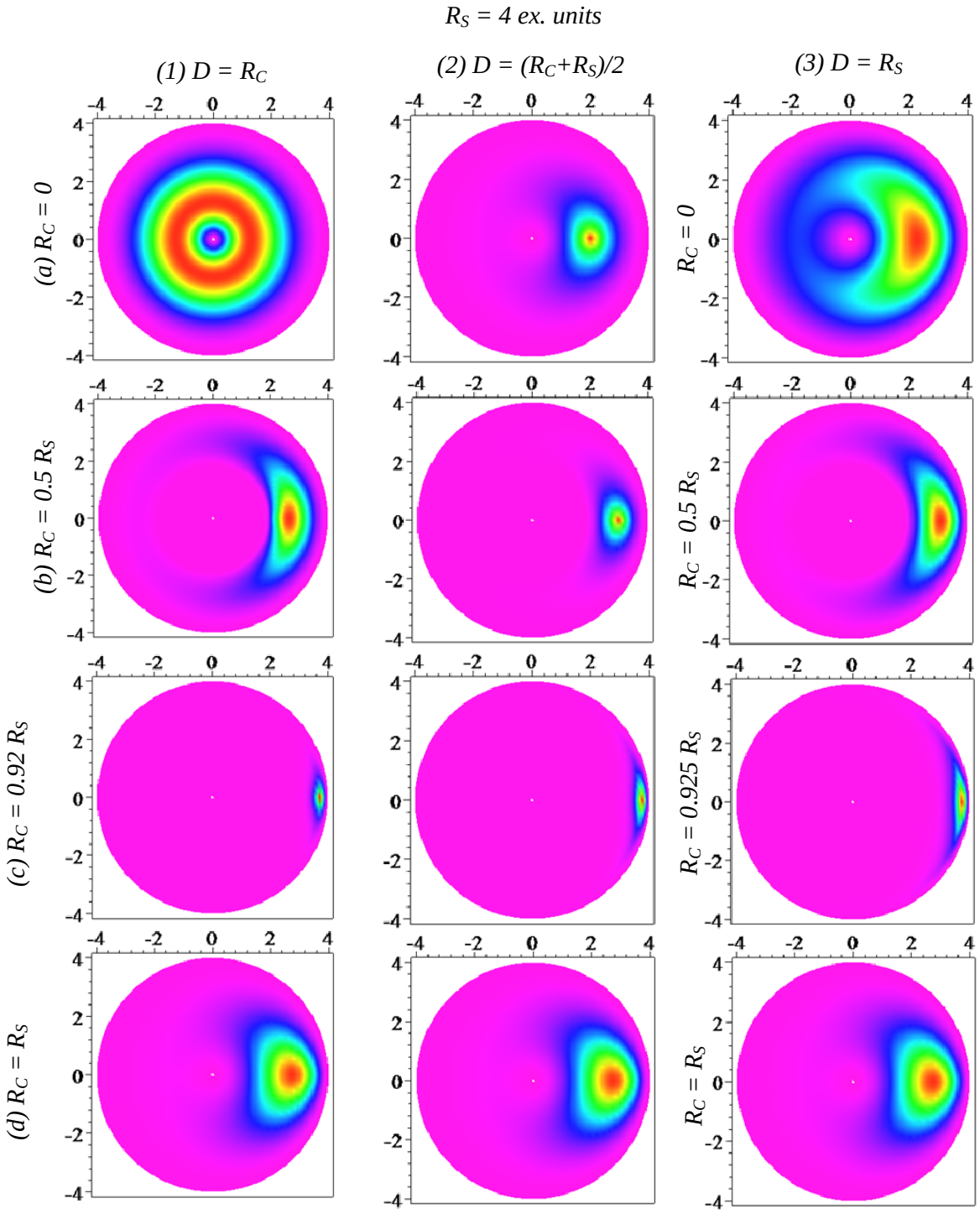


*Fig. 4: Radial probability density* $r_e^2\Psi_{D^0}^2$ *of an off-centre donor confined in a ZnS/CdSe core/shell nanostructure for a shell radius* $R_S = 4$ *ex. units, different values of core radius:* $R_C = 0(a), 0.5R_S(b), 0.92R_S(c), R_S(d)$ *and three donor positions:* $d = R_C(1), (R_C + R_S)/2(2), R_S(3)$.

## 4. Conclusion

In conclusion, ground state energy and corresponding wave function of an off-centre donor impurity placed anywhere in the well region of a ZnS/CdSe core/shell nanostructure are determined via Ritz variational principle and in the framework of the envelope function approximation. Coulomb correlation parameter, binding

energy and spatial extension of heavy-hole exciton and off centre donor are drawn as functions of core to shell radii ratio in both cases and for different ionized donor positions in case of hydrogenic donor. We showed that for nanostructures such as the thickness of spherical CdSe layer is about 1 nm, we assist to a giant electron-hole Coulomb correlation that enhances off-centre donor and heavy-hole exciton binding energies up to two times the binding energy in CdSe spherical quantum dots. Comparison of exciton and off-centre donor in different positions allowed us to say that in a first approximation, exciton can be well described as a volume hydrogenic donor at halfway between shell surfaces reminding the concept of donor-like exciton formerly proposed for an exciton confined in a spherical quantum dot.

**Acknowledgments**

Asmaa IBRAL is grateful to CNRST of Morocco for its financial support under grant N° G12/003.

## References

[1] A. I. Ekimov and A. A. Onushchenko, Pis'ma. Zh. Eksp. Teor.Fiz, **34**(6), 363 (1981).
[2] L. E. Brus, J. Chem. Phys. **79**, 5566 (1983).
[3] L. E. Brus, J. Chem. Phys. **80**(9), 4403 (1984).
[4] Zhenda Lu, Chuanbo Gao, Qiao Zhang, Miaofang Chi, Jane Y. Howe, Yadong Yin, Nano Lett. **11**(8), 3404 (2011).
[5] W. Russ Algar, Mario G. Ancona, Anthony P. Malanoski, Kimihiro Susumu, Igor L. Medintz, ACS Nano, **6**(12), 11044 (2012). DOI: 10.1021/nn304736j
[6] Roberto Trevisan, Pau Rodenas, Victoria Gonzalez-Pedro, Cornelia Sima, Rafael Sánchez Sánchez, Eva M. Barea, Ivan Mora-Sero, Francisco Fabregat-Santiago Sixto Gimenez, J. Phys. Chem. Lett., **4**(1), 141 (2013). DOI: 10.1021/jz301890m
[7] Jui-Ming Yang, Haw Yang and Liwei Lin, ACS Nano, **5**(6), 5067 (2011).
[8] Igor L. Medintz, Thomas Pons, James B. Delehanty, Kimihiro Susumu, Florence M. Brunel, Philip E. Dawson and Hedi Mattoussi, Bioconjugate Chem, **19**(9), 1785 (2008).
[9] Jianbo Liu, Xiaohai Yang, Kemin Wang, Yan He, Pengfei Zhang, Haining Ji, Lixin Jian, Wei Liu, Langmuir, **28**(28), 10602 (2012).
[10] Patrick Hoyer, Thorsten Staudt, Johann Engelhardt Stefan W. Hell, Nano Lett., **11**(1), 245 (2011).
[11] Shawn J. Tan, Nikhil R. Jana, Shujun Gao, Pranab K. Patra, Jackie Y. Ying, Chem. Mater., **22**(7), 2239 (2010).
[12] Simon Hennig, Sebastian van de Linde, Mike Heilemann and Markus Sauer, Nano Lett., **9**(6), 2466 (2009).
[13] Christina Tekle, Bo van Deurs, Kirsten Sandvig, Tore-Geir Iversen, Nano Lett., **8**(7), 1858 (2008).
[14] Sujata Sundara Rajan, Hong Yan Liu, Tania Q. Vu, ACS Nano, **2**(6), 1153 (2008).
[15] Vasudevanpillai Biju, Damodaran Muraleedharan, Ken-ichi Nakayama, Yasuo Shinohara, Tamitake Itoh, Yoshinobu Baba, Mitsuru Ishikawa, Langmuir, **23**(20), 10254 (2007).
[16] Sébastien Courty, Camilla Luccardini, Yohanns Bellaiche, Giovanni Cappello, Maxime Dahan, Nano Lett., **6**(7), 1491 (2006).
[17] D. Schooss, A. Mews, A. Eychmüller, H. Weller, Phys. Rev. B **49**(24), 17072 (1994).
[18] M. Marceddu, M. Saba, F. Quochi, A. Lai, J. Huang, D. V. Talapin, A. Mura, G. Bongiovanni, Nanotechnology **23**, 15201 (2012).
[19] S. Rawalekar, M. V. Nikhil Raj, H. N. Ghosh, Science of Advanced Materials, **4**(5-6), 637 (2012). DOI: http://dx.doi.org/10.1166/sam.2012.1331
[20] Z. Pan, H. Zhang , K. Cheng, Y. Hou, J. Hua, X. Zhong, ACS Nano, **6**(5), 3982(2012). DOI: 10.1021/nn300278z
[21] L. P. Balet, S. A. Ivanov, A. Piryatinski, M. Achermann, V. I. Klimov, Nano Letters, **4**(8), 1485 (2004). DOI: 10.1021/nl049146c
[22] S. A. Ivanov, A. Piryatinski, J. Nanda, S. Tretiak, K. R. Zavadil, W. O. Wallace, D. Werder, V. I. Klimov, J. Am. Chem. Soc., **129**, 11708 (2007).
[23] M. Schmidt, M. Grün, S. Petillon, E. Kurtz, C. Klingshirn, Appl. Phys. Lett. **77**, 85 (2000). DOI: 10.1063/1.126885
[24] Y. Shirasaki, G. J. Supran, M. G. Bawendi, V. Bulović, Nature photonics, **7**, 13 (2013).
[25] H. El Ghazi, A. Jorio, I. Zorkani, Physica B, **426**, 155 (2013).
[26] H. El Ghazi, A. Jorio, I. Zorkani, Physica B, **427**, 106 (2013).
[27] A. Mmadi, K. Rahmani, I. Zorkani, A. Jorio, Superlattices and Microstructures, **57**, 27 (2013).
[28] D. J. BenDaniel and C. B. Duke, Physical Review **152**(2), 683 (1966).
[29] A. Mukherjee, S. Ghosh, J. Phys. D: Appl. Phys., **45**, 195103 (2012).
[30] E. C. Niculescu, M. Cristea, Journal of Luminescence, **135**, 120 (2013).
[31] A. Ibral, A. Zouitine, S. Aazou, E. M. Assaid, E. M. Feddi, F. Dujardin, J. Optoelectron. Adv. Mater **15**, 1268 (2013).
[32] A. I. Ekimov, I. A. Kudryavtsev, M. G. Ivanov, Al. L. Efros, Sov. Phys. Solid State, **31**, 1385 (1989).
[33] A. I. Ekimov, I. A. Kudryavtsev, M. G. Ivanov, Al. L. Efros, Journal of luminescence, **46**, 83 (1990).
[34] E. Assaid, E. Feddi, M. Khaidar, F. Dujardin B. Stébé, Physica Scripta, **63**, 329-335 (2001).
[35] S. Nomura, T. Kobayashi, J. Appl. Phys. **75**(1), 382 (1994).
[36] A. I. Ekimov, Al. L. Efros, M. G. Ivanov, A. A. Onushenko, S. K. Shumilov, Solid State Commun. **69**, 565 (1989).

*Corresponding author : eassaid@yahoo.fr